AD

AD-E400 490

CONTRACTOR REPORT ARLCD-CR-80016

STEEL EROSION PRODUCED BY DOUBLE BASE, TRIPLE BASE, AND RDX COMPOSITE PROPELLANTS OF VARIOUS FLAME TEMPERATURES

LEONARD H. CAVENY
PRINCETON UNIVERSITY
PRINCETON, NEW JERSEY

OCTOBER 1980

US ARMY ARMAMENT RESEARCH AND DEVELOPMENT COMMAND
LARGE CALIBER
WEAPON SYSTEMS LABORATORY
DOVER, NEW JERSEY

The views, opinions, and/or findings contained in this report are those of the author(s) and should not be construed as an official Department of the Army position, policy or decision, unless so designated by other documentation.

Destroy this report when no longer needed. Do not return it to the originator.

The citation in this report of the names of commercial firms or commercially available products or services does not constitute official endorsement or approval of such commercial firms, products, or services by the United States Government.

UNCLASSIFIED

SECURITY CLASSIFICATION OF THIS PAGE *(When Date Entered)*

REPORT DOCUMENTATION PAGE

READ INSTRUCTIONS BEFORE COMPLETING FORM

1. REPORT NUMBER: Contractor Report ARLCD-CR-80016
2. GOVT ACCESSION NO.:
3. RECIPIENT'S CATALOG NUMBER:

4. TITLE *(and Subtitle)*: STEEL EROSION PRODUCED BY DOUBLE BASE, TRIPLE BASE, AND RDX COMPOSITE PROPELLANTS OF VARIOUS FLAME TEMPERATURES

5. TYPE OF REPORT & PERIOD COVERED:

6. PERFORMING ORG. REPORT NUMBER:

7. AUTHOR(s):
Leonard H. Caveny
Princeton University

8. CONTRACT OR GRANT NUMBER(s):

9. PERFORMING ORGANIZATION NAME AND ADDRESS:
Princeton University
Princeton, NJ 08540

10. PROGRAM ELEMENT, PROJECT, TASK AREA & WORK UNIT NUMBERS: 1L/62603AH18/TA12/WA03

11. CONTROLLING OFFICE NAME AND ADDRESS:
ARRADCOM, TSD
STINFO (DRDAR-TSS)
Dover, NJ 07801

12. REPORT DATE: October 1980

13. NUMBER OF PAGES: 34

14. MONITORING AGENCY NAME & ADDRESS *(if different from Controlling Office)*:
ARRADCOM, LCWSL
Applied Sciences Division (DRDAR-LCA-G)
Dover, NJ 07801

15. SECURITY CLASS. *(of this report)*: UNCLASSIFIED

15a. DECLASSIFICATION/DOWNGRADING SCHEDULE:

16. DISTRIBUTION STATEMENT *(of this Report)*

Approved for public release; distribution unlimited.

17. DISTRIBUTION STATEMENT *(of the abstract entered in Block 20, if different from Report)*

18. SUPPLEMENTARY NOTES

This report summarizes the results of a project carried out for U.S. Army ARRADCOM under Scientific Services Agreement Delivery Order 1248 administered by Battelle Columbus Laboratories.

19. KEY WORDS *(Continue on reverse side if necessary and identify by block number)*

Erosion
Erosivity
RDX composite propellant
Double base propellant
Triple base propellant
Gun barrel wear

20. ABSTRACT *(Continue on reverse side if necessary and identify by block number)*

Experimental studies of steel erosion were performed using three propellant types (i.e., double base, triple base, and RDX composite). Propellants of each type were formulated to have isochoric flame temperatures of approximately 2700, 3000, and 3300°K. The experiments (performed in a combustor that used conventional perforated grains) produced mass loss data over a range of pressure-versus-time (P-T) programs. The propellant charge weights were selected to produce rather severe melt-and-wipe-off type of erosion. The combined effects

DD FORM 1 JAN 73 1473 EDITION OF 1 NOV 65 IS OBSOLETE

UNCLASSIFIED

SECURITY CLASSIFICATION OF THIS PAGE *(When Data Entered)*

of varying the propellant type and the P-T program produce interactions which greatly complicate the interpretation of the erosion-producing processes. In an effort to relate the results to gun barrel erosion, the various propellant grains and duty cycles were compared on the basis of equivalent muzzle velocity. Hence, the erosion data were correlated in terms of the integral of P-T. For equivalent P-T integrals and flame temperatures, RDX composite propellant grains were clearly the most erosive, whereas the erosivity was less for the double and triple base propellant grains (which had similar erosivity). Within a propellant type, the hottest propellants (3300°K) generally produced mass losses twice as great as the nominal propellants (3000°K).

ACKNOWLEDGMENT

The author wishes to acknowledge the assistance rendered by Drs. Joseph A. Lannon and Arthur J. Bracuti, Applied Sciences Division, ARRADCOM.

TABLE OF CONTENTS

	Page no.
Introduction	1
Steel Erosion Measurements	2
Basis for Comparing Propellant Erosivity	2
Results	3
Discussion	4
References	6
Distribution List	

TABLES

1	Propellant compositions and thermochemical data	7
2	Erosion produced by triple base propellant	8
3	Erosion produced by nitramine (RDX) propellant	9
4	Erosion produced by double base propellant	10
5	Regression analysis of data	11

FIGURES

		Page no.
1	Cross-sectional view of the vented-combustor erosion	12
2	Typical pressure-versus-time records	13
3	Mass loss produced by triple base propellants	14
4	Mass loss produced by nitramine (RDX) propellants	15
5	Mass loss produced by double base propellants	16
6	Comparison of mass loss produced by nominal 2700 K propellants	17
7	Comparison of mass loss produced by nominal 3000 K propellants	18
8	Comparison of mass loss produced by nominal 3300 K propellants	19
9	Mass loss produced by triple base propellants on log-log plot	20
10	Mass loss produced by nitramine (RDX) propellants on log-log plot	21
11	Mass loss produced by double base propellants on log-log plot	22
12	Comparison of log-log plots of mass loss produced by nominal 3300 K propellants	23
13	Mass loss versus peak chamber pressure produced by triple base propellants	24
14	Mass loss versus peak chamber pressure produced by nitramine (RDX) propellants	25
15	Mass loss versus peak chamber pressure produced by double base propellants	26
16	Mass loss versus average molecular weight for conditions of constant P-T integral and flame temperature	27

INTRODUCTION

Steel erosion experiments were conducted using grains made from a series of specially formulated propellants*. The series consists of formulations of cool (2,700° K), nominal (3,000° K), and hot (3,300° K) double base, triple base, and RDX composite propellants. The principal ingredients in the propellants are given in table 1. Table 1 also summarizes pertinent calculated and measured properties. The propellant web thicknesses were selected so that the burning times of the propellants would be in the same range. The objectives of the experiments were to:

1. Measure the relative erosivity of the various propellant/-grain formulations.

2. Correlate the erosion data in terms of parameters which can be related to the gun performance.

Experiments in which either the propellant formulation or the pressure-versus-time (P-T) cycle are changed for the purpose of evaluating their influence on steel erosion always produce interactions which complicate the interpretation of the specific effects which produce erosion. For example, changes in propellant formulation may alter significantly propellant burning rate as well as the combustion gas composition, which, in turn, affect the rate at which the steel is heated. In particular, convective heating rates are very dependent on flame temperature as well as gas transport properties. Thus, differences in erosion as a function of propellant type must be interpreted in terms of gas composition to analyze the contributions of chemical interactions which produced changes in transport properties such as thermal conductivity and specific heat (ref 1). With respect to gun barrel erosion, the duty cycle performance in terms of muzzle velocity is a very meaningful basis for comparing the erosivity of different propellant grain types and different heating cycles. In the regime studied, the convective heating processes, rather than surface chemical attack, is the dominant heating mode and the erosion is primarily due to melt and wipe-off.

---

*Personal communication with J. A. Lannon, ARRADCOM, Dover, NJ, April 1978.

STEEL EROSION MEASUREMENTS

Erosion of steel specimens was produced using the vented combustor techniques shown in figure 1. Specimens were AISI 4340 steel 2.5 mm thick with 0.71 mm diameter orifices. The leading edge of the orifice was steamlined. The P-T cyles produced in the combustor approximate those produced by large gun chambers. Typical P-T traces are shown in figure 2. The primary measurement in these experiments was mass loss. A mass loss of 1 mg corresponds to an equivalent erosion depth of about 22 micrometers along the orifice. The propellant charge weights during the test series ranged from 0.6 to 1.4 g.

BASIS FOR COMPARING PROPELLANT EROSIVITY

Since the net effect of the imposed P-T program is to accelerate a projectile in a barrel, an effective measure of the relative energy associated with a particular P-T program is the velocity it would impart to a projectile. Without regard to barrel length and neglecting various losses, projectile velocity is approximately proportional to the integral of pressure over the action time. Thus, for a given P-T program, the relative energy associated with a particular duty cycle can be calculated without one's knowing the specifics of the gas composition, flame temperature, burning rate, surface area, etc.

Another important factor in determining the relative erosivity of various propellants and P-T programs is the dynamics of the heating from the propellant gases to the steel surface and the heat conduction to the subsurface regions. For example, if a prescribed P-T integral (and thus muzzle velocity) is achieved by using a relatively low pressure and an extended action time, the steel surface temperature can be maintained below the point where significant mass loss occurs. This situation can occur because at sufficiently low pressures (and thus low heating rates) there is ample time for heat to be conducted away from the steel surface; hence, the surface temperature remains below the melting point. Therefore, a comparison of relative erosivity must account for the dynamics of the heat transfer processes. Accordingly, the integral was evaluated between the times the pressure exceeded a threshold of 60 MPa, since below that pressure the low heating rates do not contribute significantly to the mass loss. This integral is referred to as I_{60}. In this manner the correlation is weighted toward that portion of the heating cycle which produces erosion and away from the low pressure extended time P-T programs that do not produce measurable mass losses.

While it is reasonable to compare the relative erosivity of propellants on an equivalent muzzle velocity basis, it must be kept in mind that the combined propellant and grain geometry systems are being compared rather than the propellants alone. In other words, since propellant properties (such as burning rate) and grain geometry characteristics (such as web thickness) affect the P-T history, separating the propellant effects from the grain geometry effects would require additional experiments in which the propellant formulations are held constant and the grain geometry systematically varied.

RESULTS

Four pairs of disks were subjected to the erosive conditions produced by each of the nine propellants. The data are summarized in tables 2, 3, and 4. The specimen-to-specimen variation can be observed by comparing the mass loss of specimens 1 and 2. This type of variation is typical of previous experimental series (ref 1). The fourth test in each series was performed after the results of the first three tests were analyzed. The test conditions for the fourth test were selected so as to resolve ambiguities and to broaden the data correlations. The P-T integrals were measured by using a planemeter on the oscilloscope photographic records and are accurate to within 3%.

Each of the 72 measured mass losses is plotted on mass loss versus I_{60} plots (figs. 3 through 5), and least squares lines were placed through the points shown in table 5. As indicated in table 5, a few of the data points were excluded from the correlations since they were exceptions to general trends. As expected, the relative erosivity of a particular propellant/grain type increases with increasing flame temperature. The increase in mass loss produced by going from 3,000 to 3,300° K tends to be greater than that produced by going from 2,700 to 3,000° K. However, at the lower I_{60} values the trends with increasing temperature are less distinct.

In figures 6 through 8 the mass losses for the three propellant types (double base, triple base, and RDX composite) at the same nominal flame temperatures are compared. At every temperature, the RDX containing grains produce higher mass losses. However, the higher erosivity of the RDX containing grains becomes more prominent as flame temperature increases. The mass loss differences produced by double base and triple base grains are less distinct and tend to be similar.

As part of the process of interpreting the data, the results were plotted as log mass eroded versus log I_{60} (figs. 9 through 11). As indicated in table 5, the log-log representation tends to improve the coefficient of determination, but the overall trends are the same as those shown in figures 3 through 5. Figure 12 compares the relative erosivity of the 3,300° K propellant grains; the trends are the same as those shown in figure 8.

For completeness the mass loss data were plotted as a function of peak pressure (figs. 13 through 15). The lines through the data were determined by eye. The fact that the results are systematic and reveal the same trends as those shown in figures 3 through 12 is a result of the effort of the propellant formulators to make the web burning times equal. For example, propellant grains which produce equivalent peak pressures but one-half of the burning time would produce greatly reduced mass losses.

DISCUSSION

In terms of the objective as stated in the introduction:

1. For equivalent P-T integrals, the RDX composite grains are the most erosive, whereas there is no distinct differences in erosivity of the double base and triple base grains.

2. The erosion data are generally correlated by the P-T integral for pressure greater than 60 MPa.

Even though a relatively small data sample was taken, the trends are well defined.

The specimen-to-specimen variations are an intriguing aspect of the results. Of the 36 specimen pairs, one-third had specimen-to-specimen differences of 0.5 mg or more. Since in each experiment the two specimens experienced identical P-T and combustion gas conditions, understanding the specimen-to-specimen differences is an integral part of understanding the overall erosion process. The most homogeneous propellants (the double base propellants) had the smallest specimen-to-specimen variations and the best coefficient of determinations.

Part of the research being conducted at Princeton University has related low rates of mass loss to water vapor where the steel surface remains below the melting temperature (ref 2). Under those conditions, the mass loss can be attributed to surface chemical attack. In the present test series, the mass loss is at a rela-

tively high rate and is a result of high convective heating followed by melt and wipe-off. Thus, the arguments associated with water vapor concentration and the H_2O/H_2 ratio do not apply.

As discussed in reference 2, explanations of erosion rate difference under conditions of similar P-T programs require analyses that include the dynamics of the heat conduction processes, the effects of shifting equilibrium on transport properties, etc. However, it is of interest to look for a simple correlation under conditions of nearly constant flame temperature and I_{60}. Those gases with the highest fraction of light molecular weight combustion products (or the lowest average molecular weight) will have the highest thermal conductivities. Accordingly, as shown in figures 7 through 9 and figure 16 for constant flame temperature of 3,300° K and I_{60} of 1.0 MPa-s mass loss increases as molecular weight decreases. Apparently, the desired low molecular weight for improved impetus produces a correspondingly larger increase in convective heating rate.

REFERENCES

1. L. H. Caveny, A. Gany, M. Summerfield, and J. W. Johnson, "Effect of Propellant Type on Steel Erosion," Proceedings of JANNAF 1978 Propulsion Conference, CPIA Publication 293, Vol V, February 1978, pp 285-299.

2. A. Gany, L. H. Caveny, and J. W. Johnson, "Erosion of Steel by Water-Vapor Containing High Temperature Flow," Non-Equilibrium Interfacial Transport Process, ASME, July 1979.

Table 1. Propellant compositions and thermochemical data[a]

Table 1. Propellant compositions and thermochemical data[a]

	Double base			Triple base			RDX Composite		
	1	2[b]	3	1	2[c]	3	1	2	3
Principal ingredients	Percentage								
NC (13.25%N)	66.6	69.8	73.2						
NC (12.6%N)				27.4	27.4	27.4	30.0	30.0	30.0
NG	20.0	20.0	20.0	11.0	22.0	33.0	15.6	18.3	21.1
NGu				59.6	48.6	37.6			
RDX							41.5	41.5	41.5
EC	11.1	7.9	4.5				1.5	1.5	1.5
DOP							11.2	8.5	5.6
c_p (Froz), J/mol	41.8	43.5	45.6	42.5	44.0	45.6	40.6	42.0	43.5
Thermochemical data	Calculated values								
T_f, °(K)	2705	2994	3297	2698	3004	3304	2708	3002	3307
I, (J/g)	991	1046	1093	1007	1075	1132	1078	1143	1200
Concentration (mol/kg):									
CO	21.2	19.0	16.3	12.1	11.7	11.1	20.4	18.7	16.7
H_2	8.2	6.0	4.0	7.6	5.6	4.0	11.7	9.2	6.7
H_2O	6.8	8.3	9.4	9.4	10.5	11.2	6.1	7.6	8.9
N_2	4.9	5.0	5.0	13.4	12.1	10.7	8.0	8.2	8.4
CO_2	2.6	3.5	4.8	2.2	2.9	3.9	1.6	2.1	2.8
Total, mol/kg	44.1	42.0	39.9	44.9	32.1	41.2	47.9	45.8	43.6
M_w, (g/g-mol)	22.7	23.8	25.1	22.3	23.2	24.2	20.9	21.8	22.9
H_2O/H_2	0.83	1.38	2.35	1.24	1.88	2.80	0.52	0.83	1.33
	Measured values								
HEX (J/g)	3456	3803	4205	3607	3883	4427			
Web (in.)	0.023	0.026	0.032	0.020	0.028	0.034	0.021	0.025	0.030

[a]Calculated by BLAKE Code
[b]Similar to M26 propellant
[c]Similar to M30 propellant

Table 2. Erosion produced by triple base propellant

Propellant	Test	Charge Weight (g)	Peak press. (MPa)	Mass loss (mg)		Pressure Integral* (MPa-s)
				Spec 1	Spec 2	
TB-2	2	0.9825	214	1.31	2.20	0.953
	3	1.2445	310	3.28	3.25	1.187
	4	1.4150	379	3.90	4.18	1.159
	31	0.7480	145	0.81	0.65	0.469
TB-1	5	0.9868	204	1.37	1.36	0.883
	6	1.2440	331	3.26	2.32	1.241
	7	1.3769	344	4.00	3.52	1.257
	32	1.1133	269	2.07	1.90	1.149
TB-3	8	0.9700	231	4.24	3.58	0.909
	9	1.2002	314	6.58	5.36	1.009
	10	1.3907	386	7.81	8.65	1.115
	33	0.6645	128	2.08	1.76	0.549

*Integral is for time period when pressure exceeds 60 MPa.

Table 3. Erosion produced by nitramine (RDX) propellant

Propellant	Test	Charge Weight (g)	Peak Press. (MPa)	Mass loss (mg) Spec 1	Mass loss (mg) Spec 2	Pressure Integral* (MPa-s)
N-2	11	0.9817	248	3.87	3.41	0.875
	12	1.1987	341	4.93	5.58	1.078
	13	0.8369	176	2.09	2.06	0.527
	34	0.8800	203	2.30	2.91	0.840
N-1	14	0.9878	234	2.07	1.91	0.897
	15	1.1177	300	3.21	3.20	1.076
	17	1.2414	355	4.45	4.30	1.078
	35	0.8991	200	2.25	2.22	0.812
N-3	18	0.9859	248	6.16	5.60	0.881
	19	1.1672	321	8.30	6.60	1.009
	20	0.8388	186	4.98	4.48	0.701
	36	0.6492	117	1.73	1.68	0.479

*Integral is for time period when pressure exceeds 60 MPa.

Table 4. Erosion produced by double base propellant

Propellant	Test	Charge Weight (g)	Peak Press. (MPa)	Mass loss (mg)		Pressure Integral* (MPa-s)
				Spec 1	Spec 2	
DB-2	21	0.9872	238	2.30	2.77	0.978
	22	1.1122	290	3.60	4.00	1.111
	23	1.3030	362	5.36	5.28	1.178
	37	0.7776	162	1.00	0.80	0.716
DB-1	24	0.9861	224	2.43	2.66	0.917
	26	1.3973	379	4.31	4.87	1.210
	27	1.2589	3.17	3.45	3.69	1.033
	38	0.8280	176	0.74	0.92	0.797
DB-3	28	0.9875	231	4.14	4.33	0.890
	29	1.2162	317	6.08	6.47	1.006
	30	0.8342	159	2.42	2.98	0.619
	39	0.6090	117	0.81	0.64	0.474

*Integral is for time period when pressure exceeds 60 MPa.

Table 5. Regression analysis of data[a]

Propellant	Power curve $[m = a\ (I_{60})^b]$			Linear regression $(m = a + bI_{60})$		
	r^2	a	b	r^2	a	b
TB-2	0.878	2.468	1.700	0.804	-1.397	4.081
TB-1	0.979	1.638	1.495[b]	0.970	-0.876	2.526[b]
TB-3	0.918	5.764	1.941	0.850	-4.237	10.323
N-2	0.770	4.137	1.204	0.783	-1.222	5.561
N-1	0.718	3.078	2.168	0.704	-3.666	6.852
N-3	0.946	7.789	1.946	0.935	-3.074	10.45
DB-2	0.980	2.780	3.468	0.917	-5.699	8.856
DB-1	0.854	2.647	3.966	0.939	-5.919	8.898
DB-3	0.910	6.439	2.626[c]	0.951	-3.567	9.436

[a]Definitions: r^2 is coefficient of determination.

I_{60} is pressure integral for the period in which pressure is greater than 60 MPa.

m is mass loss in grams.

[b]Mass loss above 3.0 mg excluded from correlation.

[c]Data from test 29 excluded from correlation.

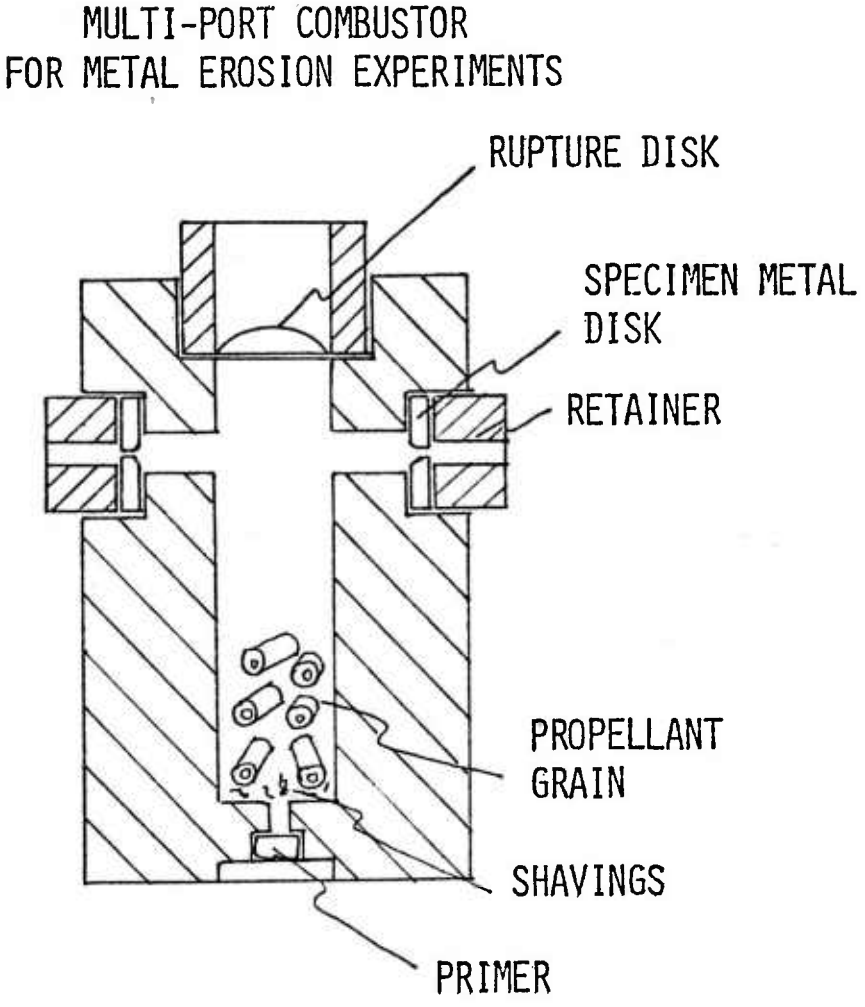

Figure 1. Cross-sectional view of the vented-combustor erosion

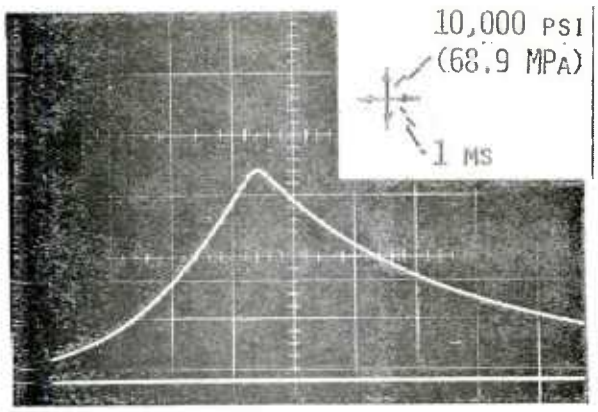

A) PROPELLANT DB-2 TEST 21
P_{MAX} = 238 MPA, I_{50} = 0.978 MPA-S

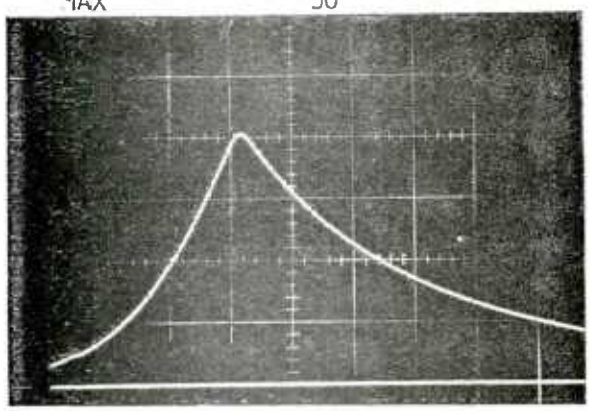

B) PROPELLANT DB-2 TEST 22
P_{MAX} = 290 MPA, I_{60} = 1.11 MPA-S

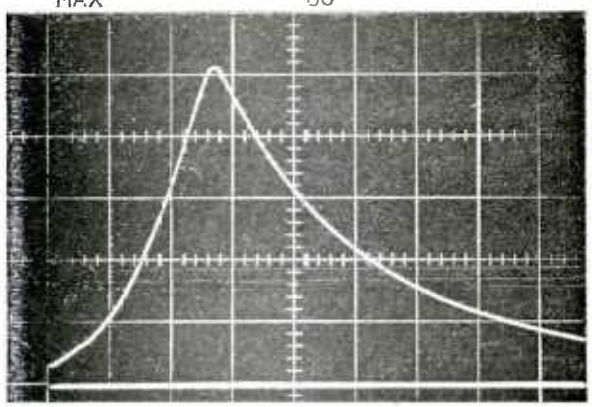

C) PROPELLANT DB-2 TEST 23
P_{MAX} = 362 MPA, I_{60} = 1.18 MPA-S

Figure 2. Typical pressure-versus-time records

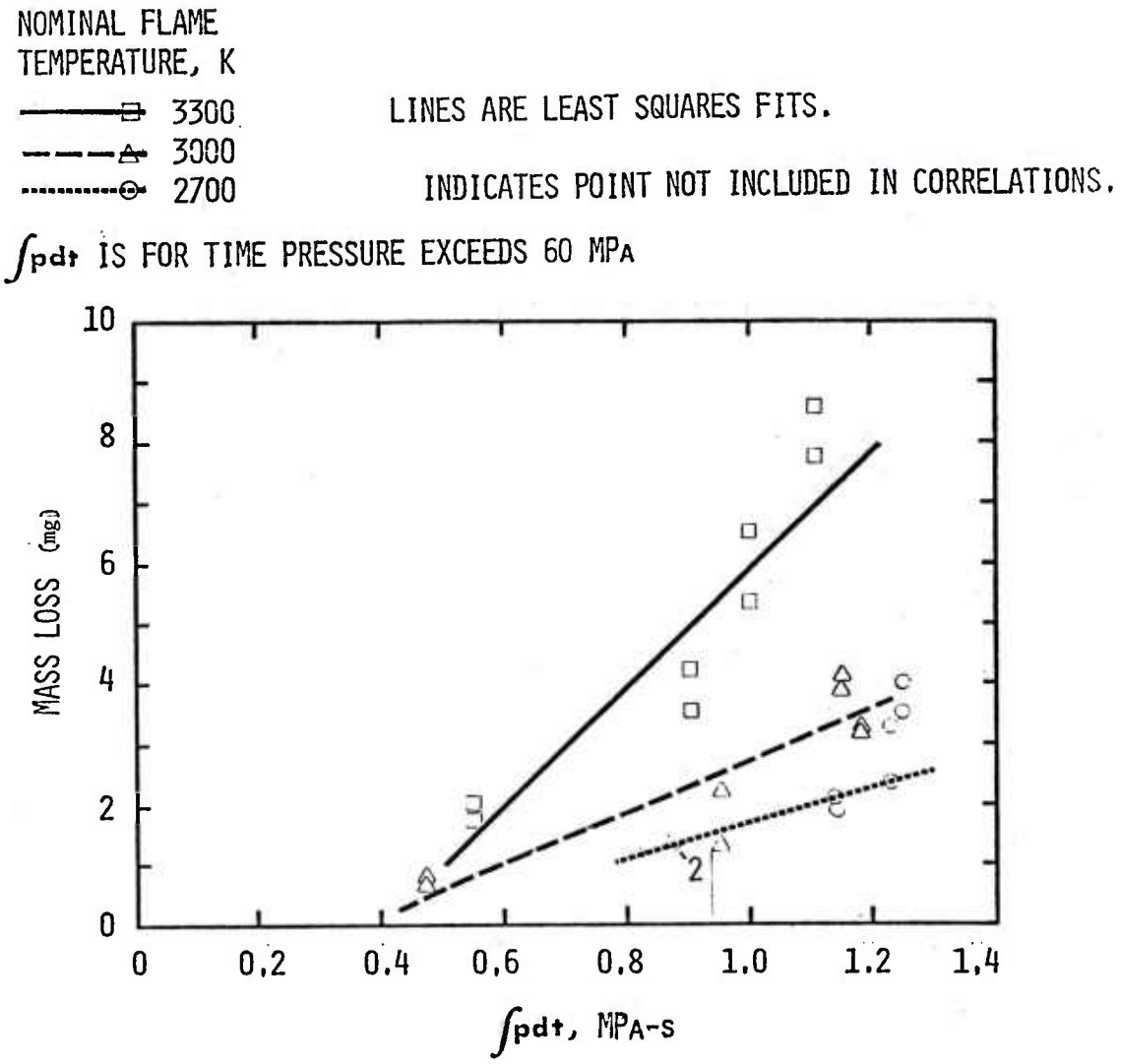

Figure 3. Mass loss produced by triple base propellants

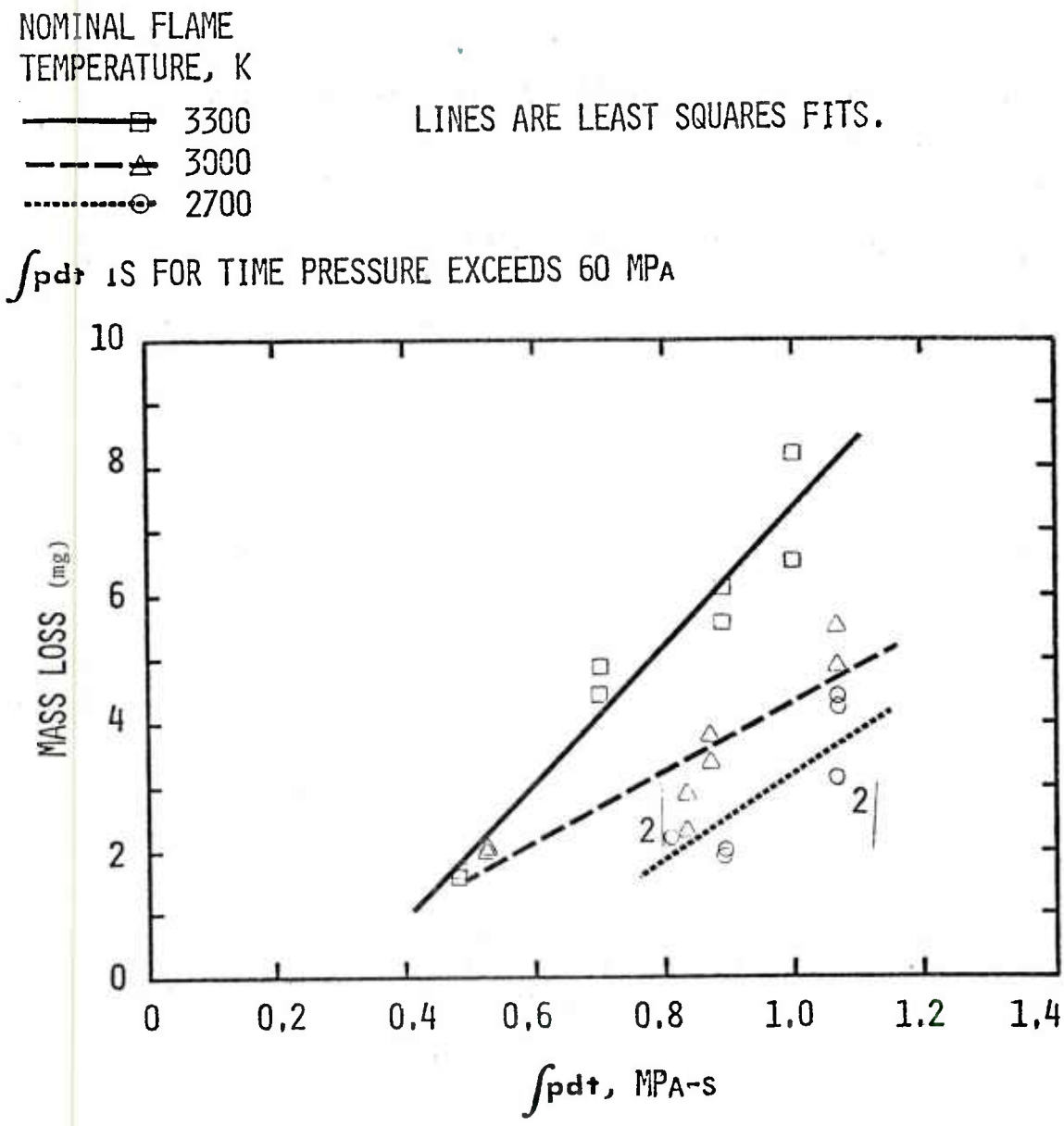

Figure 4. Mass loss produced by nitramine (RDX) propellants

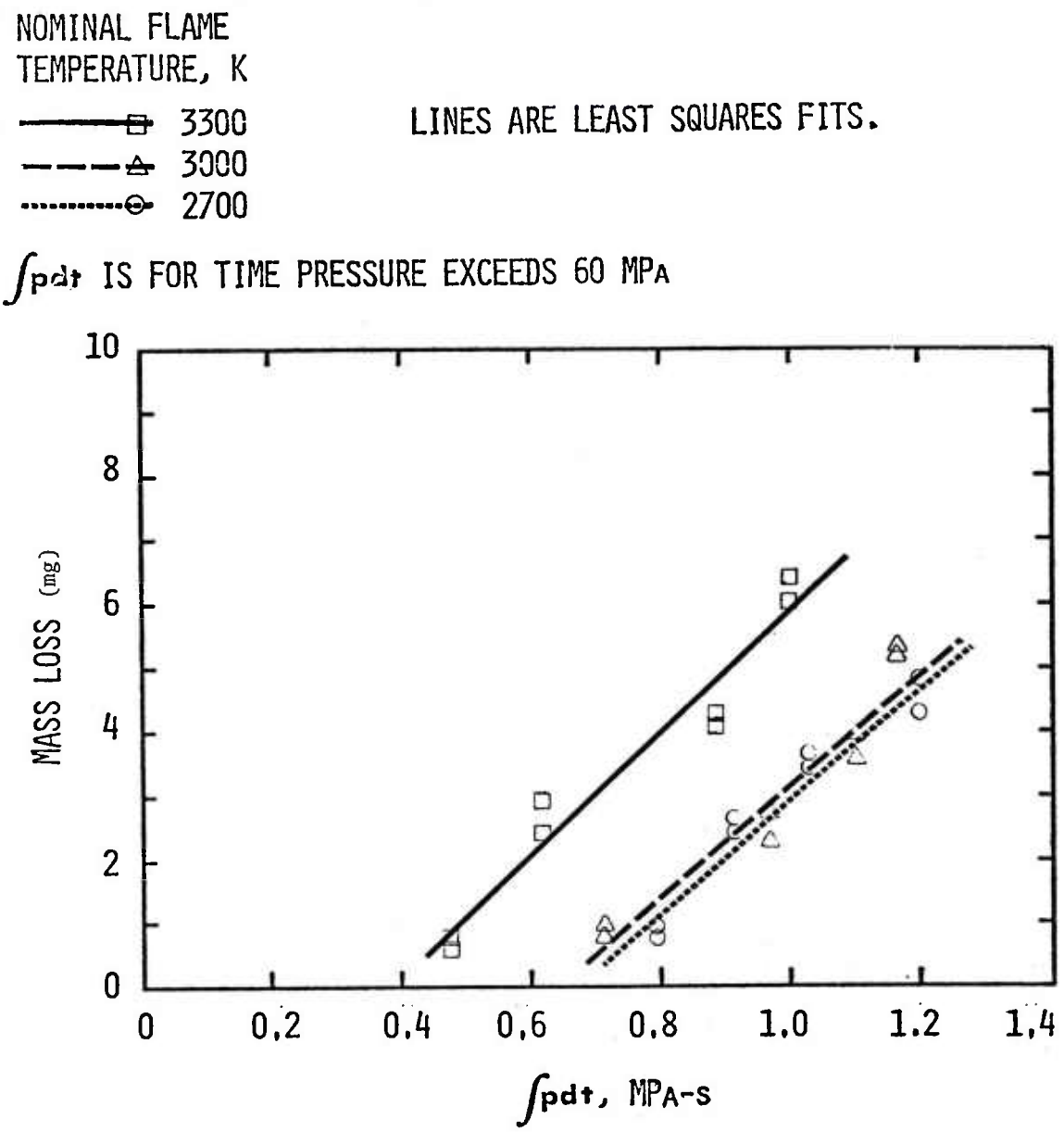

Figure 5. Mass loss produced by double base propellants

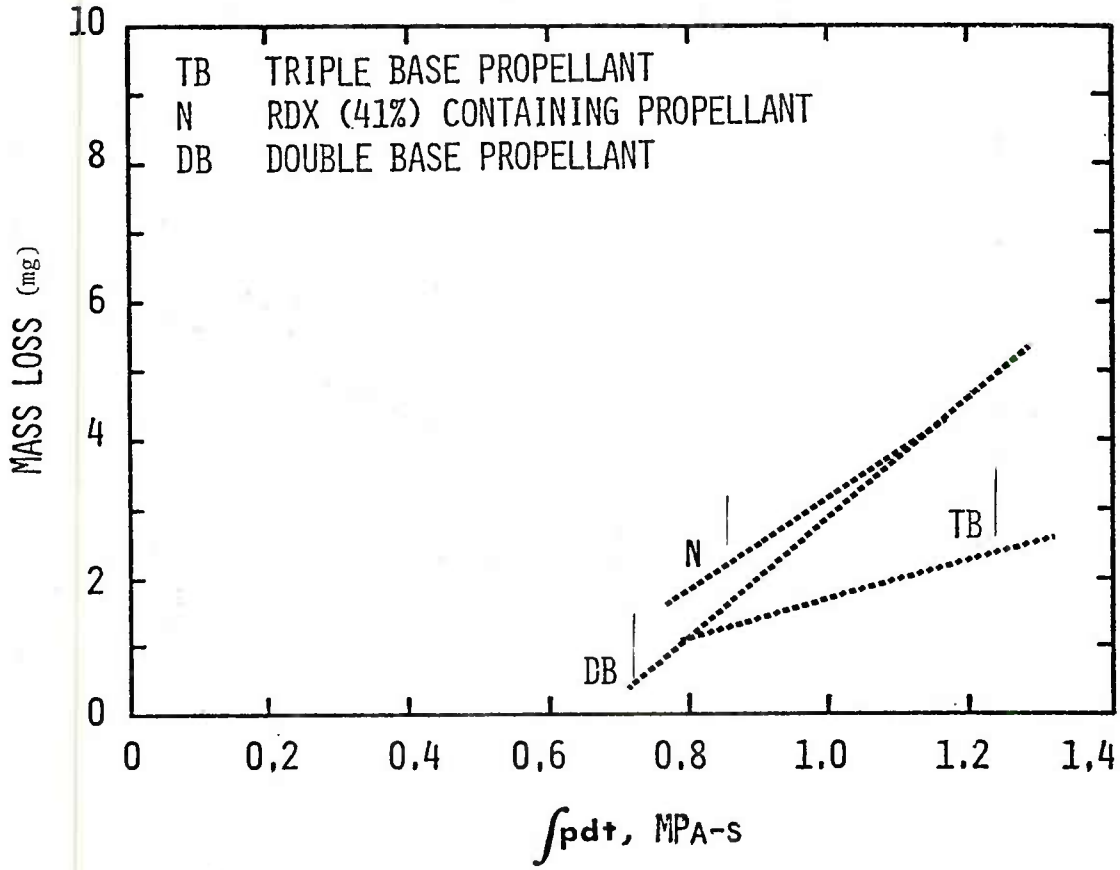

Figure 6. Comparison of mass loss produced by nominal 2700 K propellants

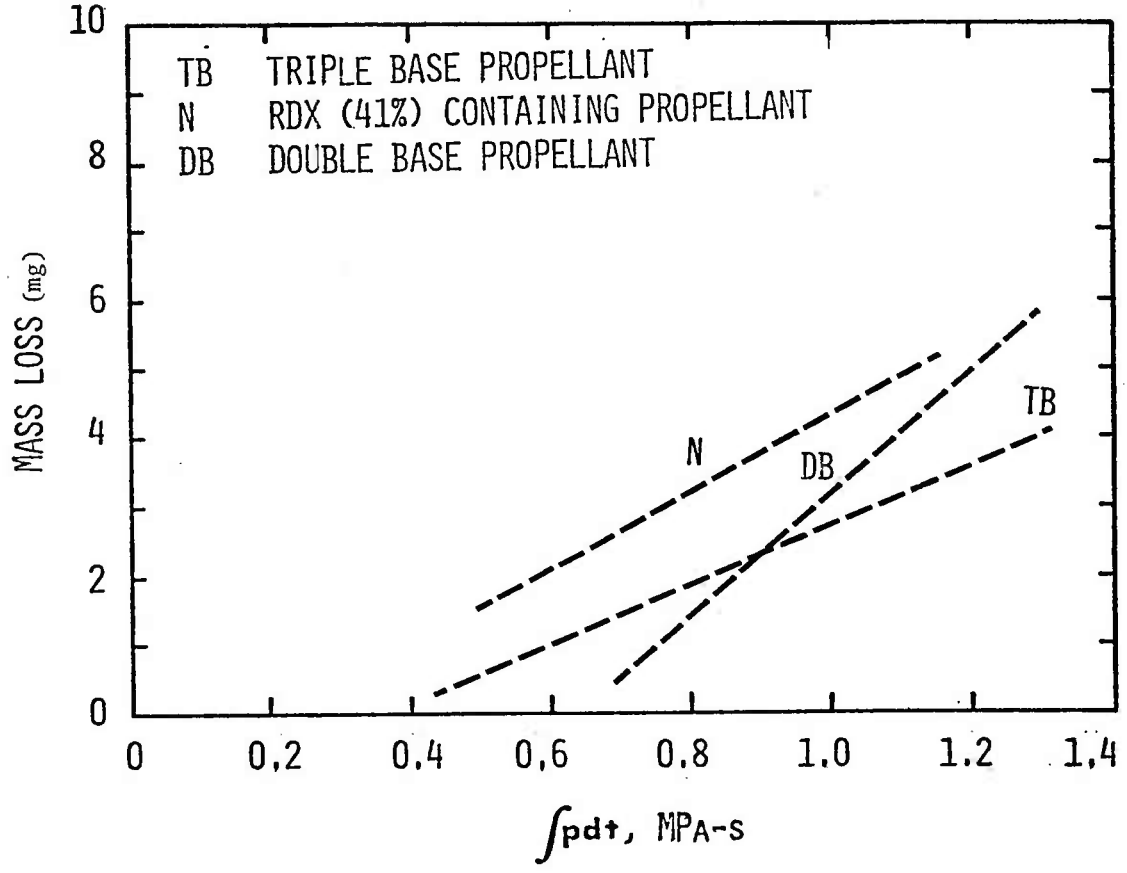

Figure 7. Comparison of mass loss produced by nominal 3000 K propellants

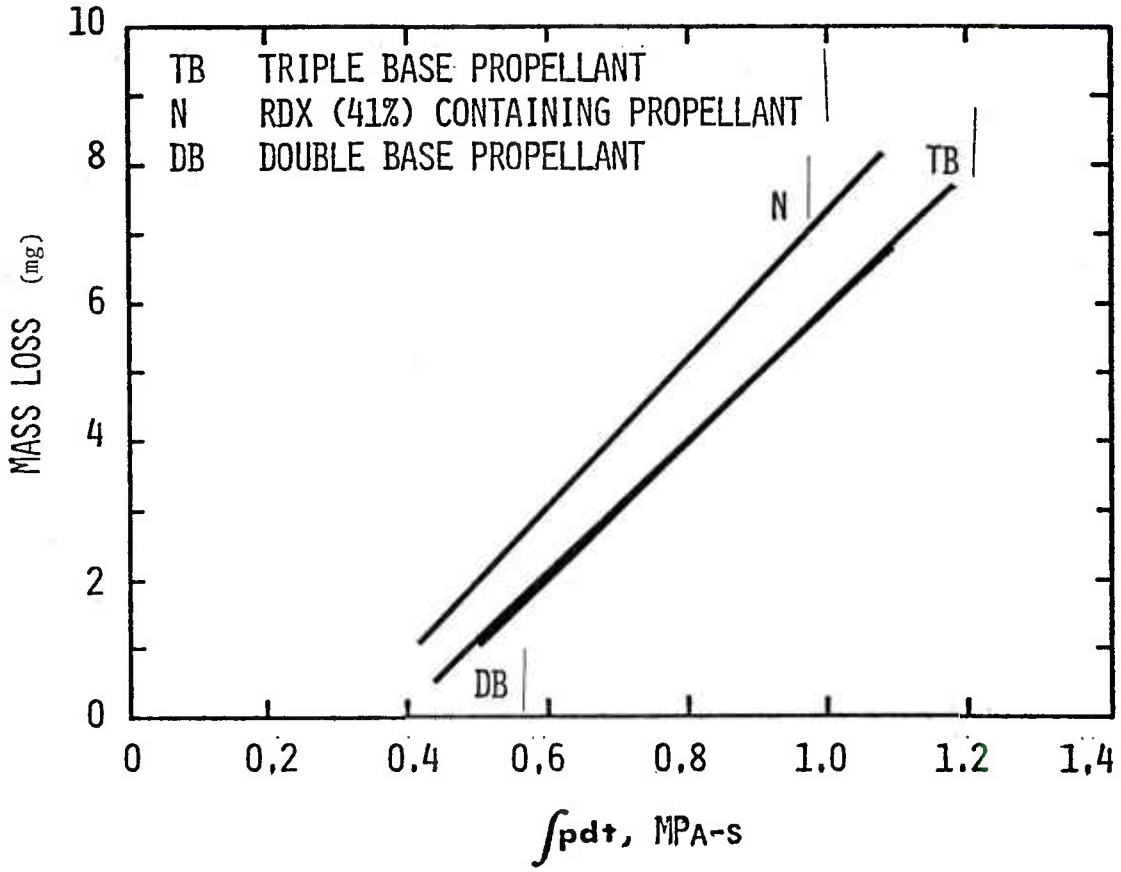

Figure 8. Comparison of mass loss produced by nominal 3300 K propellants

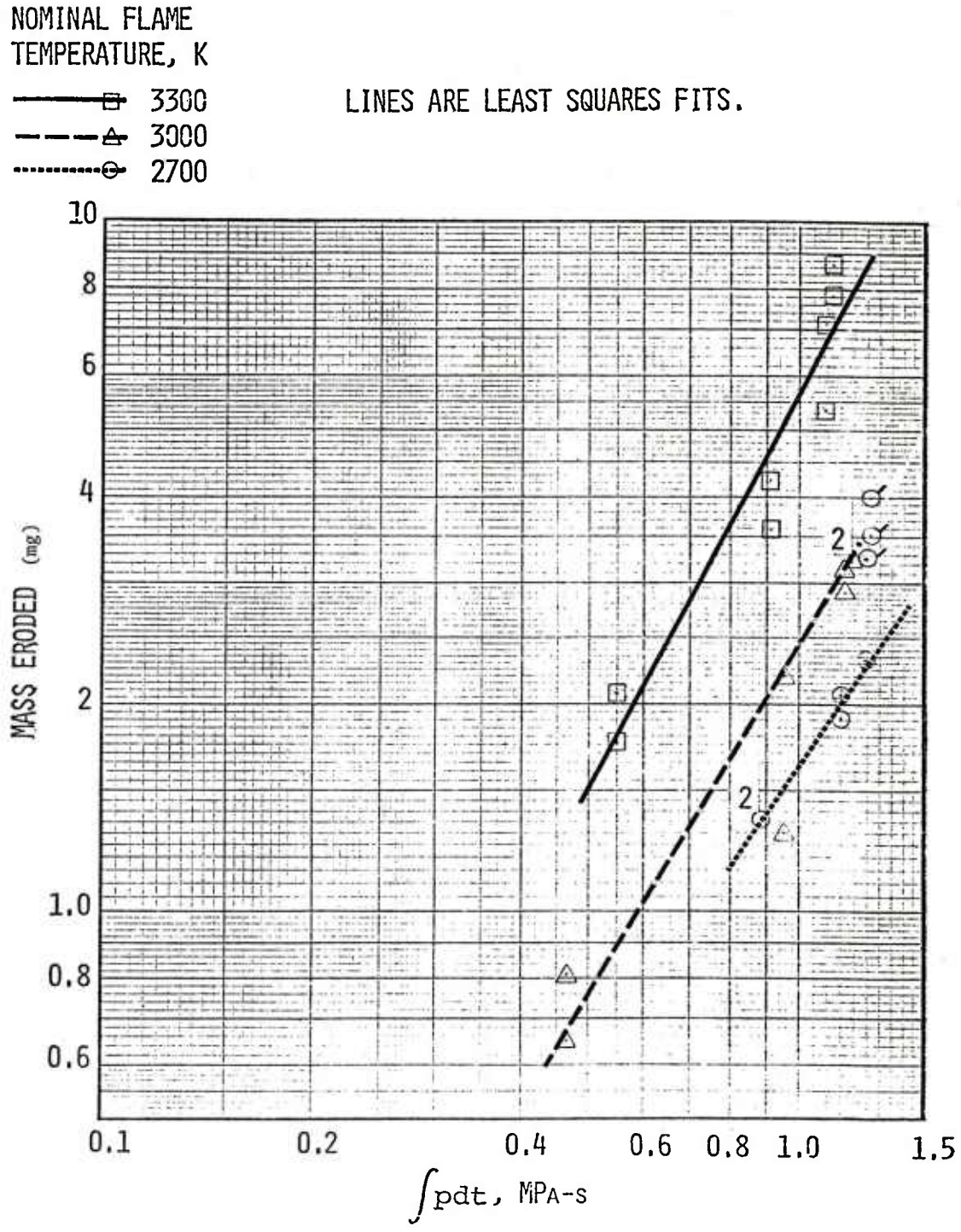

Figure 9. Mass loss produced by triple base propellants on log-log plot

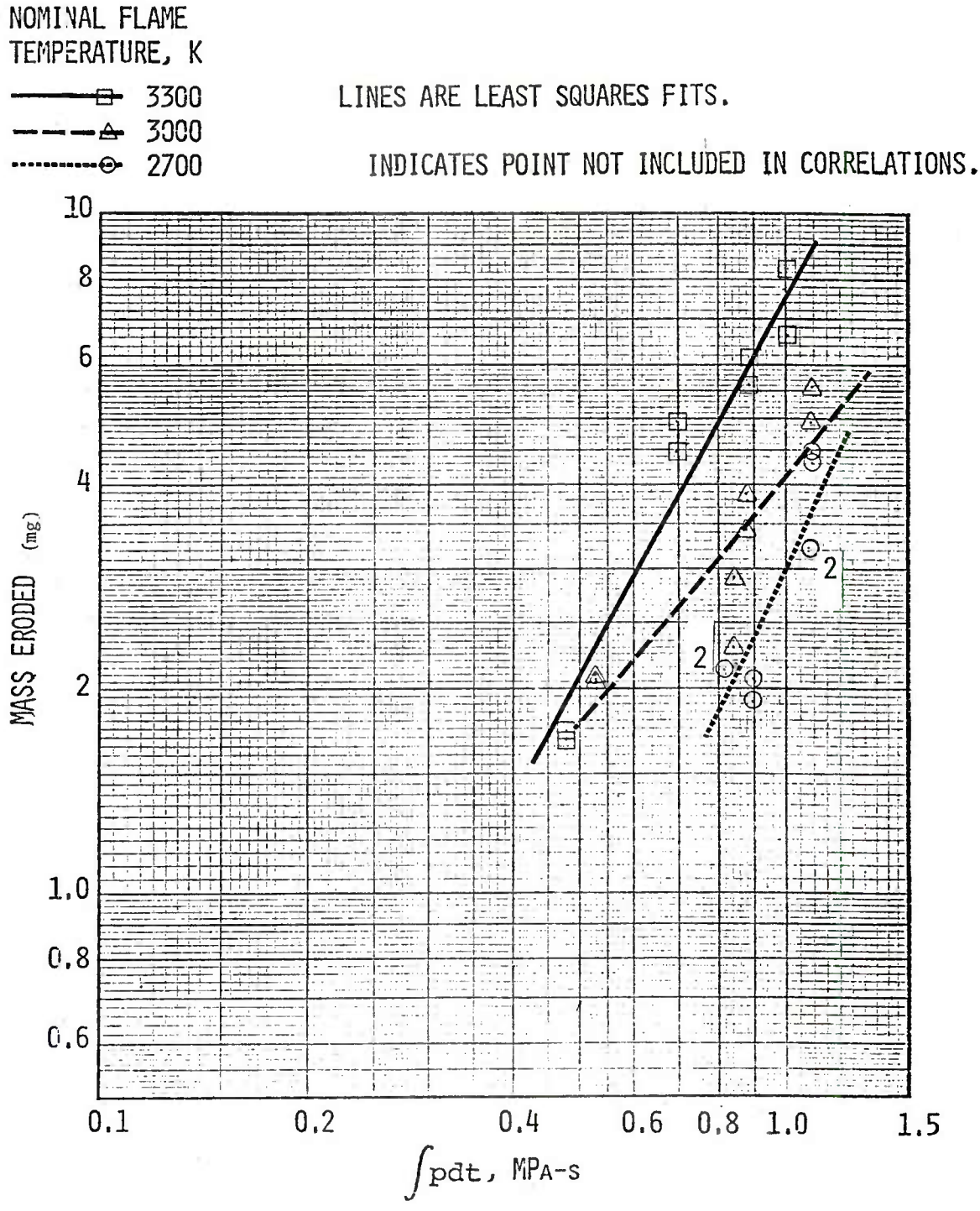

Figure 10. Mass loss produced by nitramine (RDX) propellants on log-log plot

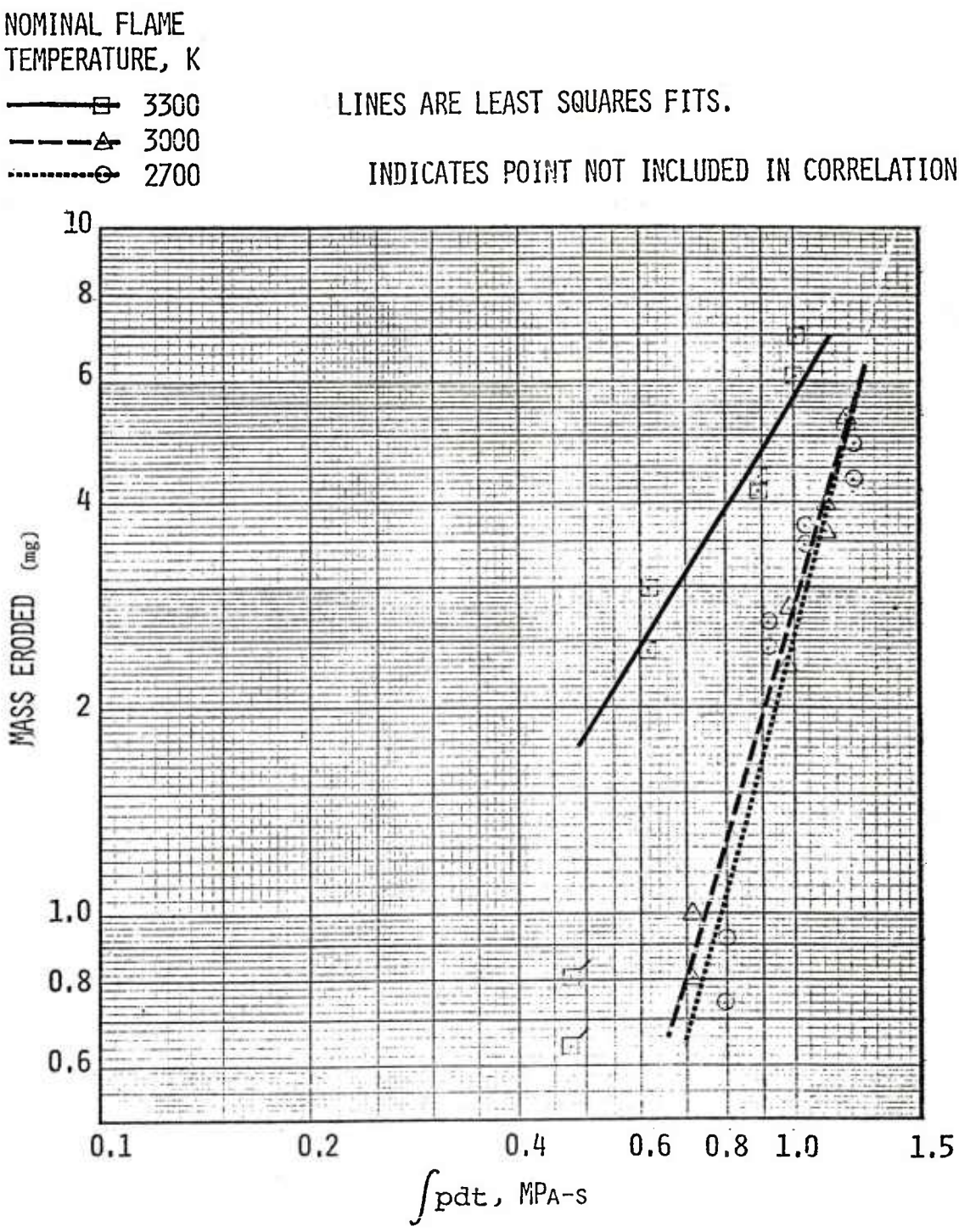

Figure 11. Mass loss produced by double base propellants on log-log plot

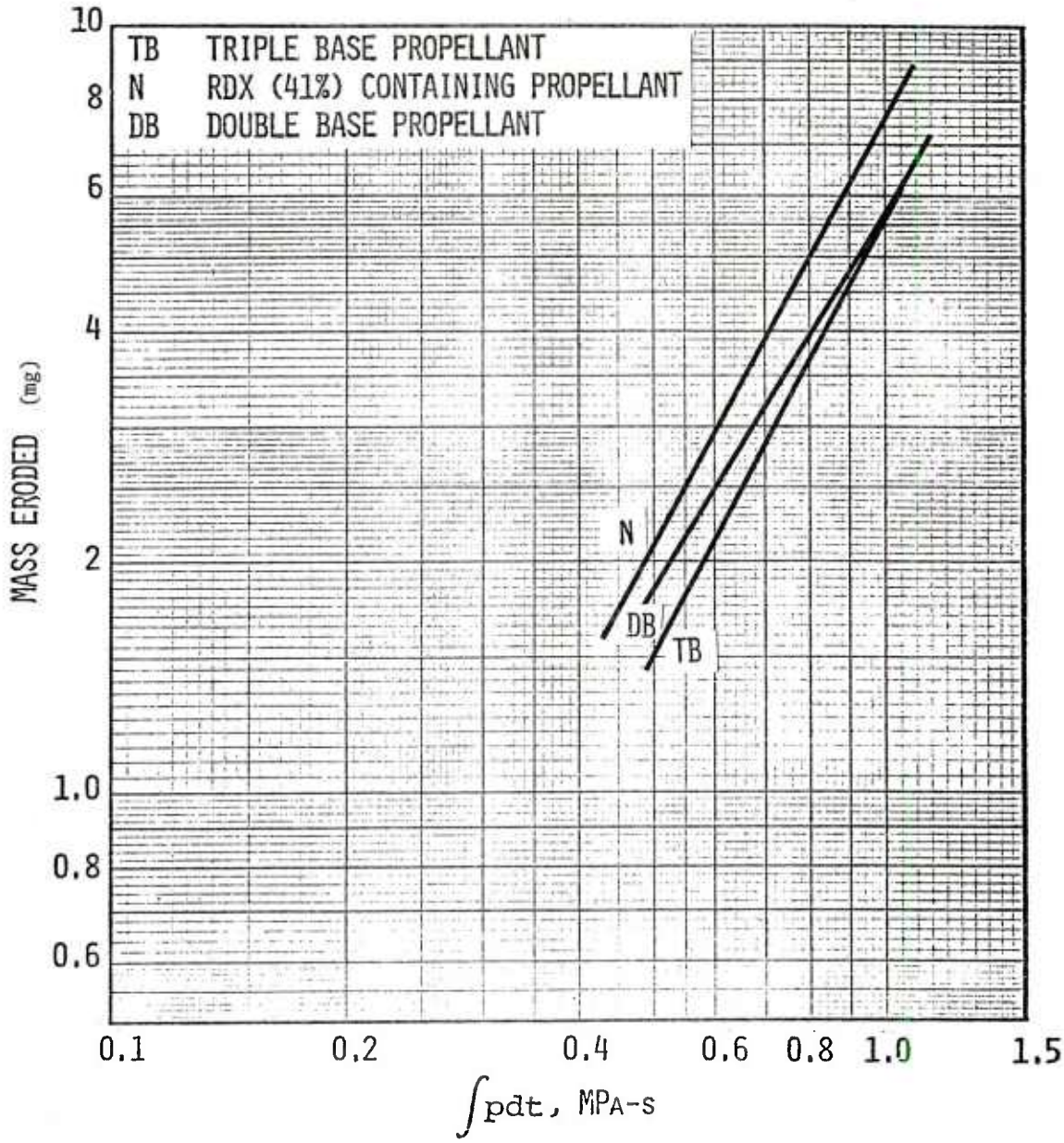

Figure 12. Comparison of log-log plots of mass loss produced by nominal 3300 K propellants

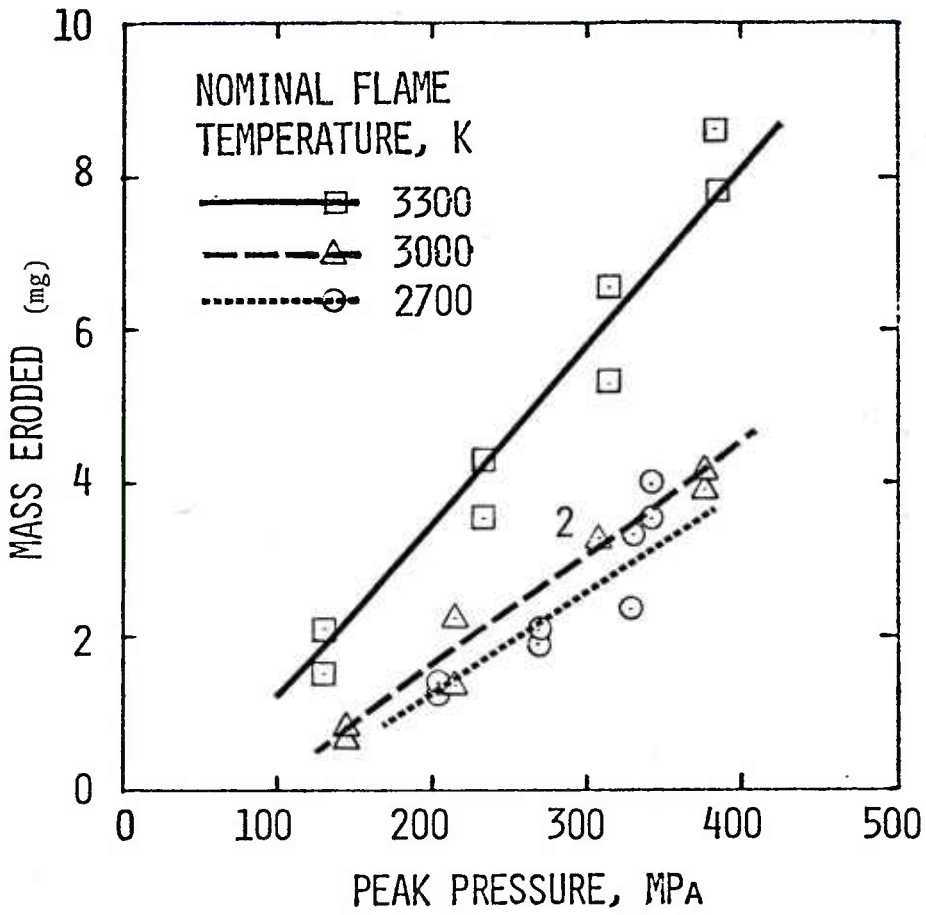

Figure 13. Mass loss versus peak chamber pressure produced by triple base propellants

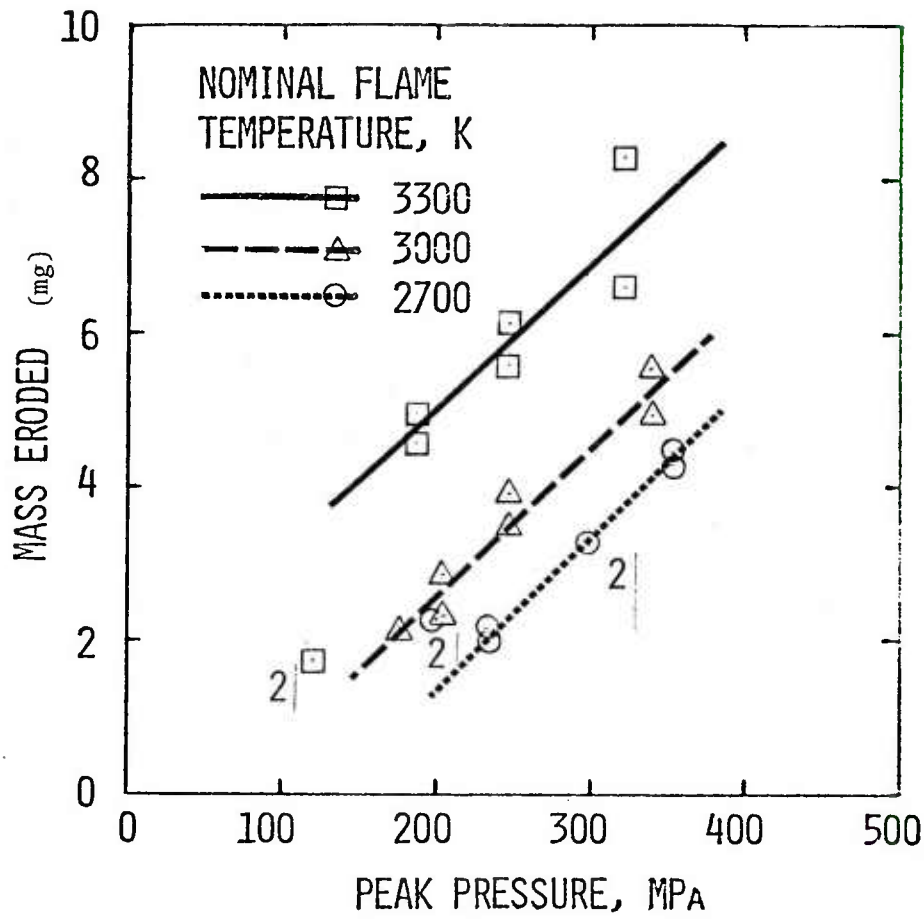

Figure 14. Mass loss versus peak chamber pressure produced by nitramine (RDX) propellants

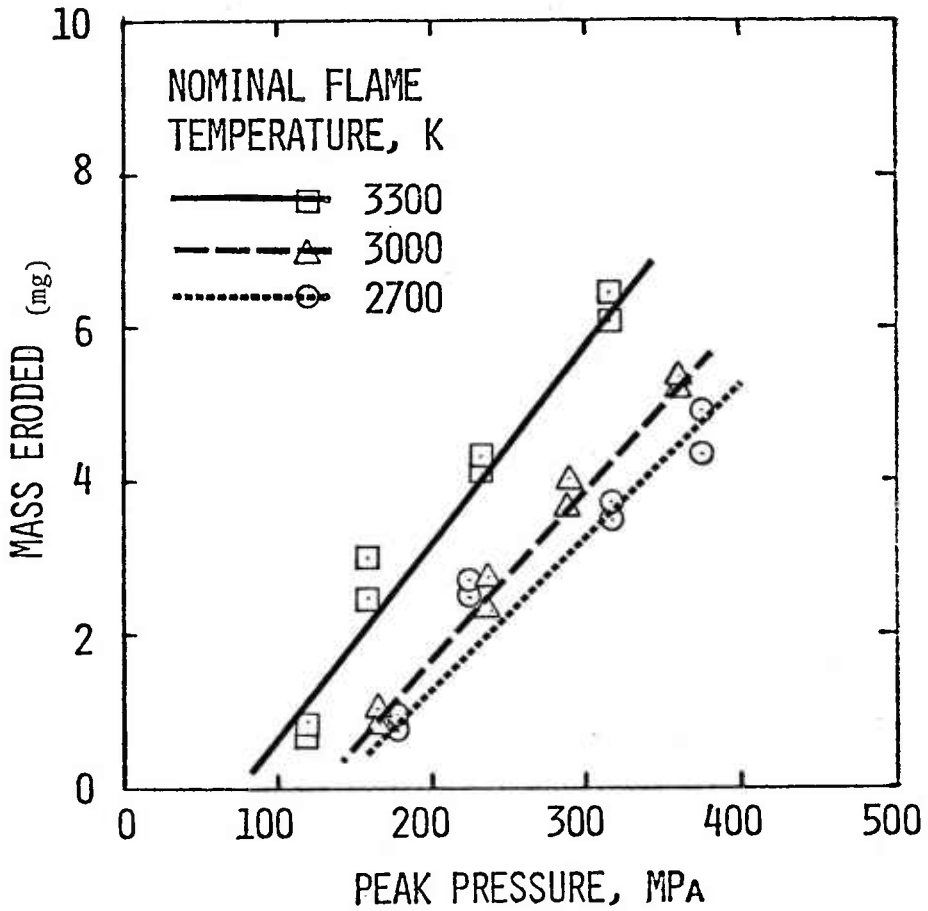

Figure 15. Mass loss versus peak chamber pressure produced by double base propellants

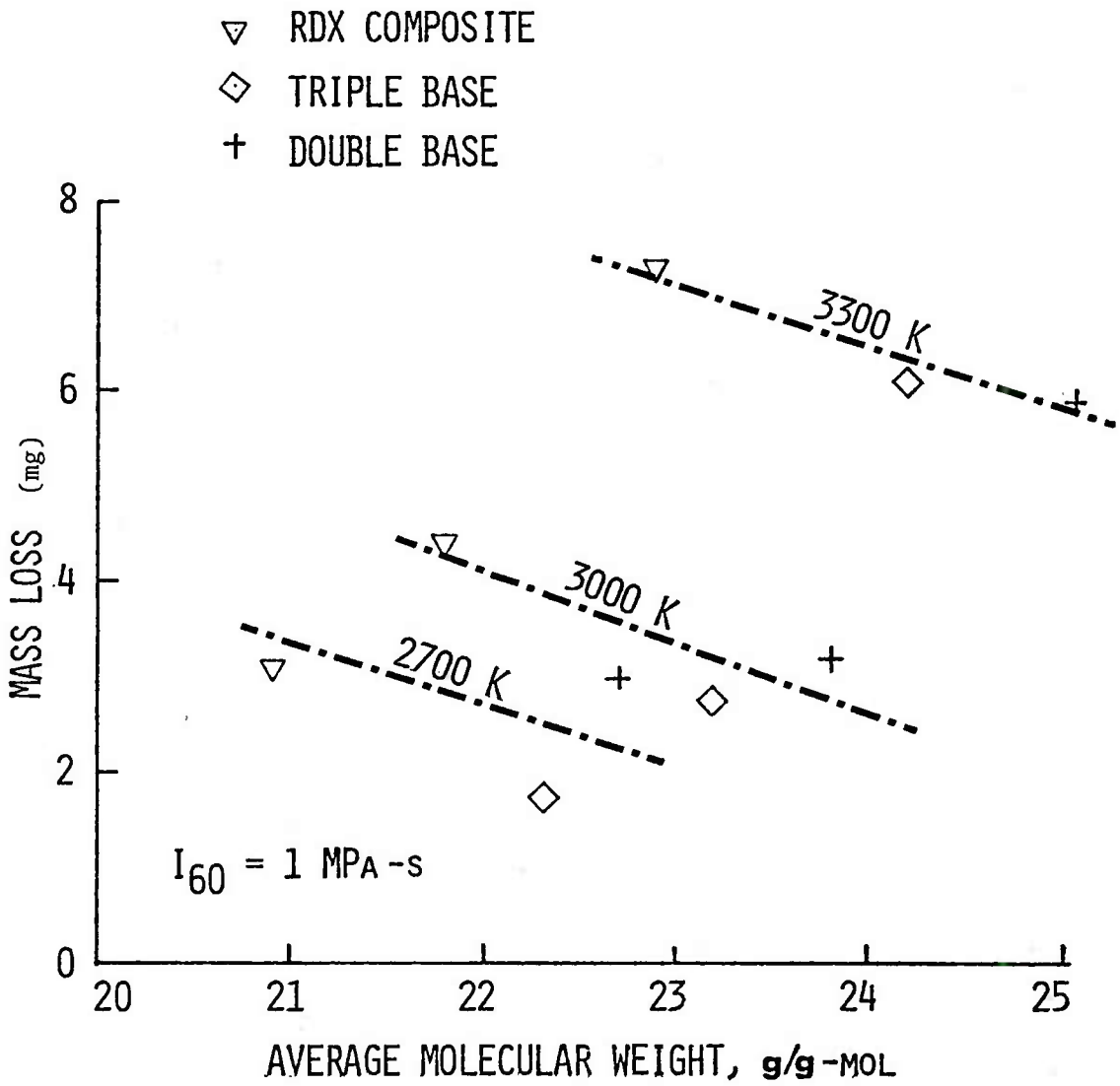

Figure 16. Mass loss versus average molecular weight for conditions of constant P-T integral and flame temperature

DISTRIBUTION LIST

Commander
US Army Armament Research and
Development Command
ATTN: DRDAR-LC, J. Frasier
DRDAR-LCA, H. Fair
DRDAR-LCA-G, L. Bottei
DRDAR-LCA-G, A. Bracuti (25)
DRDAR-LCA-G, B. Bernstein
DRDAR-LCA-G, D. Downs
DRDAR-LCA-G, L. Harris
DRDAR-LCA-G, J. Lannon
DRDAR-LCA-G, K. Russell
DRDAR-LCA-G, E. Wurzel
DRDAR-LCE, J. Picard
DRDAR-LCE, A. Stearn
DRDAR-LCS-D, J. Houle
DRDAR-LCS-D, K. Rubin
DRDAR-LCU, A. Moss
DRDAR-LCU-CA, D. Costa
DRDAR-LCU-CP, R. Corn
DRDAR-LCU-CT, E. Barrieres
DRDAR-LCU-EE, D. Ellington
DRDAR-MAD-C
DRDAR-QA, J. Rutkowski
DRDAR-SC, B. Brodman
DRDAR-SC, S. Cytron
DRDAR-SC, D. Gyorog
DRDAR-SC, H. Kahn
DRDAR-SC, L. Stiefel
DRDAR-TSE-O
DRDAR-TSS (5)
Dover, NJ 07801

Chief
Benet Weapon Laboratory
US Army Armament Research and
Development Command
ATTN: DRDAR-LCB, I. Ahmad
DRDAR-LCB, W. Austin
DRDAR-LCB, J. Busuttil
DRDAR-LCB, T. Davidson
DRDAR-LCB, G. Friar
DRDAR-LCB, R. Montgomery
DRDAR-LCB, J. Santini

DRDAR-LCB, J. Zweig
DRDAR-LCB-TL
Watervliet, NY 12189

Headquarters, Department of the Army
ATTN: DAMA-ARZ
DAMA-ARZ-A, M. Lasser
DAMA-ARZ-A, E. Lippe
DAMA-CSM
DAMA-WSW
The Pentagon
Washington, DC 20301

Director
US Army Research Office
ATTN: P. Parrish
E. Saibel
R. Husk
D. Squire
P.O. Box 12211
Research Triangle Park, NC 27709

Commander
US Naval Surface Weapons Center
ATTN: M. Shamblen
J. O'Brasky
C. Smith
L. Russell
T. W. Smith
Dahlgren, VA 22448

Commander
US Naval Ordnance Station
ATTN: S. Mitchell
Indian Head, MD 20640

Commander
Naval Surface Weapons Center
Dahlgren, VA 22448

Commander
US Naval Ordnance Station
ATTN: F. Blume
Louisville, KY 40202

Battelle Columbus Laboratory
ATTN: G. Wolken
Columbus, OH 43201

Commander
Armaments Development and Test Center
ATTN: AFATL, O. Heiney
Eglin Air Force Base, FL 32542

Lawrence Livermore Laboratory
ATTN: A. Buckingham
Livermore, CA 94550

Calspan Corporation
ATTN: G. Sterbutzel
P.O. Box 235
Buffalo, NY 14221

Director
Chemical Propulsion Information Agency
Johns Hopkins University
ATTN: T. Christian
Johns Hopkins Road
Laurel, MD 20810

Commander
US Army Missile Research and
Development Command
ATTN: Technical Library
Redstone Arsenal, AL 35809

Weapon System Concept Team/CSL
ATTN: DRDAR-ACW
APG Edgewood Area, MD 21010

Commander
US Army Test and Evaluation Command
ATTN: DRSTE-AD
DRSTE-AR
DRSTE-CM-F
DRSTE-FA
DRSTE-TO-F
Aberdeen Proving Ground, MD 21005

Project Manager, M60 Tanks
US Army Tank and Automotive Command
28150 Dequindre Road
Warren, MI 48090

Director
US Army Balistic Research Laboratories
ARRADCOM
ATTN: DRDAR-TSB-S
DRDAR-BL, Dr. Eichelberger
DRDAR-BLP, L. Watermeier
DRDAR-BLP, J. R. Ward
DRDAR-BLP, I. C. Stobie
DRDAR-BLP, I. W. May
DRDAR-BLP, J. M. Frankle
DRDAR-BLP, T. L. Brosseau
Aberdeen Proving Ground, MD 21005

Project Manager
Cannon Artillery Weapons Systems
ATTN: DRCPM-CAWS
Dover, NJ 07801

Commander
US Army Armament Materiel Readiness Command
ATTN: DRSAR-HA, J. Turkeltaub
DRSAR-HA, S. Smith
DRSAR-LEP-L
DRCPM-TM
Rock Island, IL 61299

Program Manager XM1 Tank System
ATTN: DRCPM-GCM-SI
Warren, MI 48090

Project Manager
Tank Main Armament Systems
ATTN: DRCPM-TMA-TM
Dover, NJ 07801

Project Manager
Division Air Defense Gun
ATTN: DRCPM-ADG
Dover, NJ 07801

Director
US Army Materials and Mechanics Research Center
ATTN: J. W. Johnson
R. Katz
Watertown, MA 02172

Director
US Army TRADOC Systems Analysis Activity
ATTN: ATAA-SL, Tech Library
White Sands Missile Range, NM 88002

Commander
US Army Air Defense Center
ATTN: ATSA-SM-L
Fort Bliss, TX 79916

Defense Technical Information Center (12)
Cameron Station
Alexandria, VA 22314

Director of Defense Research and Engineering
ATTN: R. Thorkildsen
The Pentagon
Arlington, VA 20301

Defense Advanced Research Projects Agency
ATTN: Director, Materials Division
1400 Wilson Boulevard
Arlington, VA 22209

Commander
US Army Materiel Development and Readiness Command
ATTN: DRCDMD-ST
DRCLDC, T. Shirata
5001 Eisenhower Avenue
Alexandria, VA 22333

Commander
US Army Tank Automotive Research and
Development Command
ATTN: DRDTA-UL
Warren, MI 48090

Princeton Combustion Research Labs, Inc.
ATTN: N. Messina
1041 U.S. Highway One North
Princeton, NJ 08540

Technical Library
ATTN: DRDAR-CLJ-L
APG Edgewood Area, MD 21010

US Army Materiel Systems Analysis Activity
ATTN: DRXSY-MP
Aberdeen Proving Ground, MD 21005